1688B

Boundary Formation in the Developing Heart: The Role of BAF Subunit Smarcc1a

Ivy Fernandes, Heidi J. Auman, and Deborah Yelon
Division of Biological Sciences, University of California, San Diego, La Jolla, CA, USA

The atrioventricular canal is a specialized region of the zebrafish heart

The atrioventricular canal (AVC) is a specialized cardiac territory that forms at the junction between the atrial and ventricular chambers. The AVC is morphologically and molecularly distinct from the adjacent cardiac chambers, and the specific properties of the AVC are necessary for proper cardiac function. Conductive properties within the AVC myocardium create a pause between the atrial and ventricular heartbeats; additionally, the AVC endocardium forms cushions that will later remodel into valve leaflets. Despite the functional importance of AVC development, we do not fully understand the molecular mechanisms that initially pattern this region.

Figure 1. By 48 hpf, the zebrafish AVC (purple) has formed distinct morphological and molecular properties. Both the myocardium, the outer muscular layer depicted in pink, and the endocardium, the inner endothelial layer depicted in green, express a set of "AVC genes" that are not found in the adjacent chambers.

Loss-of-function mutation in *smarcc1a* disrupts cardiac form and function

To decipher the mechanisms that define the AVC boundary, we are interested in identifying zebrafish mutations that disrupt cardiac patterning and morphology. Here, we focus on a loss-of-function mutation in the *smarcc1a* gene: in *smarcc1a* mutants, the heart fails to display looped and expanded cardiac chambers and instead appears relatively linear (Fig. 2C,D).

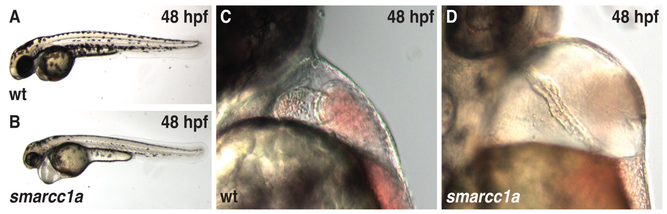

Figure 2. Loss-of-function mutation in *smarcc1a* results in a linear heart at 48 hpf. (A,B) In comparison to wild-type embryos (wt), *smarcc1a* mutant embryos have a slightly shorter body axis, decreased pigmentation, pericardial edema, and a thickened yolk extension. (C,D) At 48 hpf, cardiac chambers are misshapen and relatively linear in *smarcc1a* mutants.

Smarcc1a encodes a subunit of the SWI/SNF ATP-dependent chromatin remodeling complex

The causative mutation within the *smarcc1a* gene creates a premature stop codon that truncates the protein within its SANT domain, a protein-protein interaction domain that is thought to be essential for Smarcc1a function (Fig. 3A,B). Smarcc1a is a subunit of the SWI/SNF ATP-dependent chromatin remodeling complex (Fig. 3C). To identify how a mutation of *smarcc1a* results in a linear heart, we investigated the mutant phenotype during three major developmental transitions: the establishment of the cardiac progenitor population, the assembly of the heart tube, and the process of cardiac looping and chamber expansion.

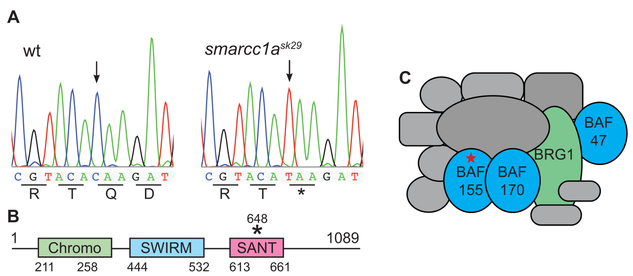

Figure 3. The *smarcc1a* mutation results in a premature stop codon within the SANT domain. (A) *smarcc1a* mutants contain a C to T transition at position 1942 of the *smarcc1a* open reading frame (arrows), resulting in a premature stop codon. (B) Zebrafish *smarcc1a* encodes a 1089 amino acid protein with several conserved motifs and approximately 74% overall similarity to human SMARCC1. The *smarcc1a* mutation changes Gln648 (CAA) to a stop codon (TAA), disrupting the SANT domain. (C) Illustration of the SWI/SNF complex with the catalytic subunit Brg1 marked in green, core subunits marked in blue and BAF155, the mamallian homolog of the zebrafish Smarcc1a subunit, marked with a star. Adapted from Gatchalian et al., 2018.

Normal cardiac progenitor formation in *smarcc1a* mutants

To assess the formation of the cardiac progenitor population in *smarcc1a* mutants, we examined the expression of *nkx2.5* in the ALPM (Fig. 4A,B). Additionally, we examined the progression of myocardial differentiation by examining *myl7* expression in the bilateral populations of differentiated cardiomyocytes (Fig. 4C,D). Both progenitor formation and myocardial differentiation appear normal in *smarcc1a* mutants.

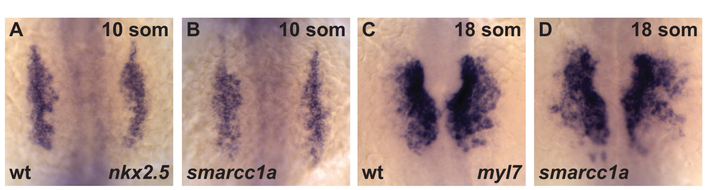

Figure 4. Cardiomyocytes differentiate normally in *smarcc1a* mutants. *In situ* hybridization depicts the expression of *nkx2.5* (A,B) and *myl7* (C,D) in the ALPM at the 10 and 18 somite (som) stages. Dorsal views, anterior to the top. (A,B) The overall location and size of the *nkx2.5* expression domain in *smarcc1a* mutant embryos is indistinguishable from that of wild-type embryos. (C,D) *smarcc1a* mutants do not exhibit defects in the formation of *myl7*-expressing differentiated cardiomyocytes.

Normal heart tube assembly, but defective chamber morphogenesis, in *smarcc1a* mutants

The initial assembly of the heart tube appears to proceed normally in *smarcc1a* mutants. At 30 hpf, both wild- type and *smarcc1a* mutant embryos exhibit a heart tube expressing *myl7* (Fig. 5A,D). Furthermore, the patterns of *vmhc* and *amhc* expression indicate normal establishment of chamber identity (Fig. 5B,C,E,F). By 48 hpf, however, looping and the formation of the AVC seem aberrant in *smarcc1a* mutants (Fig. 5G-L).

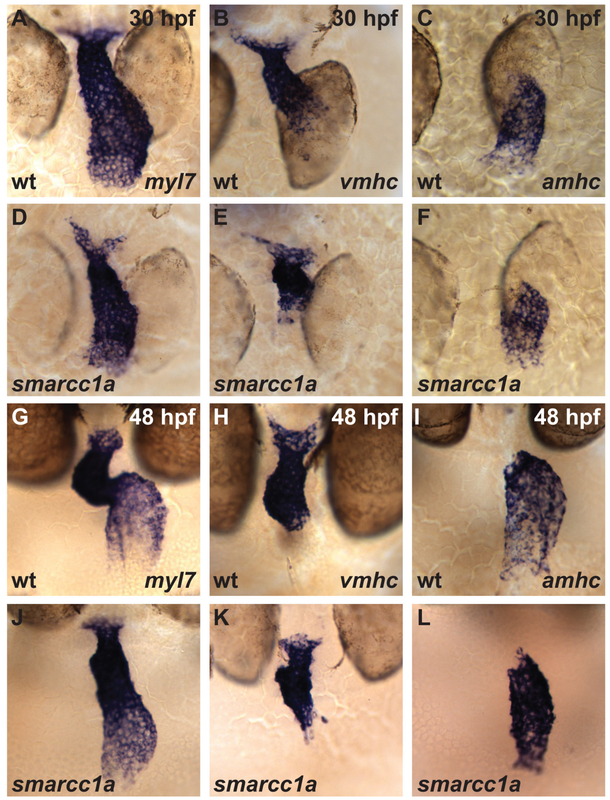

Figure 5. Looping and expansion of the linear heart tube fail to occur in *smarcc1a* mutants. *In situ* hybridization depicts the expression of *myl7* in wt (A,G) and *smarcc1a* mutants (B,J) at heart tube stages (A,D) and as chamber formation proceeds (G,J). *In situ* hybridization of *myl7* in all cardiomyocytes reveals expanded chambers and an AVC constriction in wild-type embryos at 48 hpf and a lack thereof in *smarcc1a* mutants. Expression of *ventricular myosin heavy chain* (*vmhc*) and *atrial myosin heavy chain* (*amhc*) are found in complementary domains corresponding to the ventricle and the atrium in both wild-type embryos and *smarcc1a* mutants at heart tube stages (B,C,E,F) and as chamber formation proceeds (H,I,K,L).

Smarcc1a is required for regional changes in cell morphology during chamber emergence

Regional changes in cardiomyocyte morphology fail to occur within the *smarcc1a* mutant hearts. Consistent with the abnormal shape of the mutant ventricle, ventricular cardiomyocytes in *smarcc1a* mutants fail to elongate and appear relatively round (Fig. 6C,F). These findings indicate aberrant chamber maturation and morphogenesis in the context of *smarcc1a* loss-of-function.

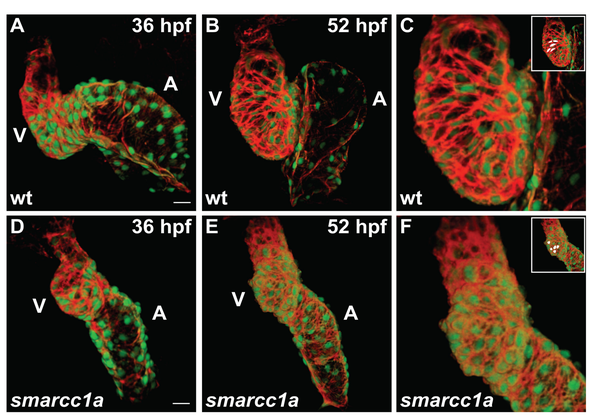

Figure 6. Cardiac chamber morphogenesis is abnormal in *smarcc1* mutants. Phalloidin staining (red) outlines cells of wild-type (A-C) and *smarcc1a* mutant (D-F) hearts expressing *Tg(myl7:egfp)*. During looping and chamber emergence, the wild-type ventricle (V) and atrium (A) come into a side-by-side alignment, whereas the *smarcc1a* mutant chambers retain a linear arrangement (A,B,D,E). Wild-type chamber emergence is accompanied by the appearance of elongated cardiomyocytes in the outer curvature of the ventricle (C) (Auman et al., 2007). *smarcc1a* mutant ventricular cardiomyocytes fail to elongate and instead retain rounded cell surfaces (F). Enlarged views of the ventricles shown in (B,E); insets show representative cell shapes filled in white (C,F).

Smarcc1a is required to hone gene expression patterns at the atrioventricular canal

During the process of cardiac looping and chamber expansion, the expression of several genes in both the endocardium and myocardium becomes refined to the AVC. However, in *smarcc1a* mutants, this refinement fails to occur. *bmp4*, a myocardial gene, and *notch1b*, an endocardial gene, are both expressed throughout the wild-type ventricle at 38 hpf and become selectively expressed at the AVC by 48 hpf (Fig. 7A,C,E,G). In *smarcc1a* mutant embryos, initial patterning appears relatively normal (Fig. 7B,F). However, by 48 hpf, both *bmp4* and *notch1b* fail to become restricted to the AVC and retain broad expression patterns (Fig. 7D,H).

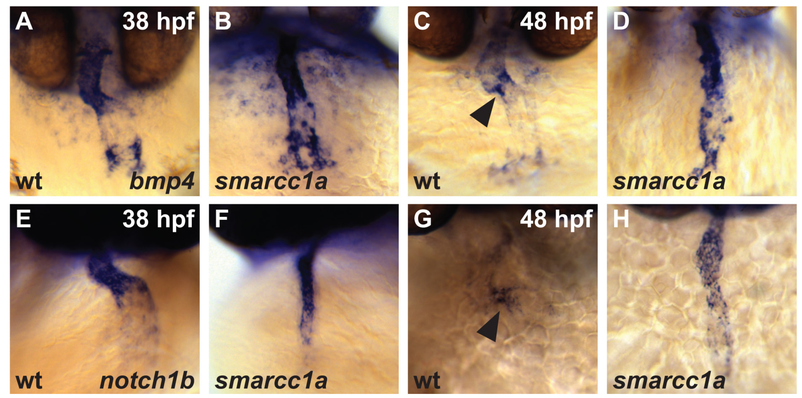

Figure 7. *In situ* hybridization compares expression patterns of *bmp4* and *notch1b* during the period of chamber emergence. (A,B) At 38 hpf, the expression of *bmp4* in *smarcc1a* mutant embryos resembles that of wt. (C,D) However, at 48 hpf, expression of *bmp4* refines to the AVC in wt (arrowhead in C), and this does not occur in *smarcc1a* mutant embryos (D). (E-H) A similar trend is seen for *notch1b*.

Smarcc1a is required to restrict expression of *tbx2b* to the atrioventricular canal

We hypothesize that Smarcc1a-containing BAF complexes act to hone specific gene expression patterns to the AVC. We are interested in identifying pathway components that act downstream of Smarcc1a to promote proper AVC patterning. We are investigating *tbx2b* as a candidate pathway component, because mouse Tbx2 has been demonstrated to promote the expression of AVC genes and to repress the expression of genes associated with the emerging chambers. *tbx2b* expression is normally spatially confined to the AVC as early as 36 hpf (Fig. 8A,C). Interestingly, our preliminary data suggests that *tbx2b* is ectopically expressed throughout the *smarcc1a* mutant heart as early as 36 hpf and persisting thereafter (Fig. 8B,D).

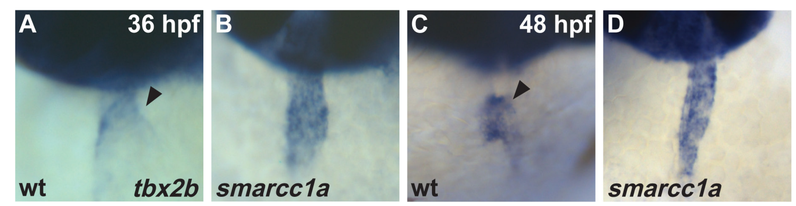

Figure 8. *tbx2b* is misexpressed throughout the *smarcc1a* mutant heart. (A-D) *tbx2b in situ* hybridization in frontal view at 36 hpf and 48 hpf. At 36 hpf, *tbx2b* expression is already restricted to the wild-type AVC (arrowheads in A,C), but is found throughout the *smarcc1a* mutant heart (B). This broad expression pattern persists at 48 hpf (D).

Working Model and Future Directions

Taken together, our preliminary data suggest a model in which Smarcc1a-containing BAF complexes define the AVC boundary by honing gene expression to the AVC, thereby defining AVC dimensions. This function of Smarcc1a-containing BAF complexes may be mediated by regulation of *tbx2b* expression.

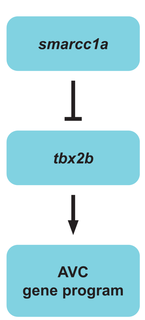

Figure 9. Illustration of the proposed model for the regulation of AVC patterning by Smarcc1a-containing BAF complexes.

To further interrogate this model and to better understand the mechanism of *smarcc1a* function, we are interested in addressing the following open questions:

- What are the pathway components that act downstream of Smarcc1a-containing BAF complexes?
- In which tissue(s) does Smarcc1a act?
- How does a specific loss of Smarcc1a function compare to a general loss of the entire SWI/SNF complex?